

Accepted Manuscript

Synthesis and physicochemical characterisation of two lead(II) complexes with O-, N-donor ligands. Lone pair functionality and crystal structure

Joanna Masternak, Barbara Barszcz, Maciej Hodorowicz, Oleksiy V. Khavryuchenko, Alina Majka

PII: S1386-1425(14)01165-2
DOI: <http://dx.doi.org/10.1016/j.saa.2014.07.084>
Reference: SAA 12504

To appear in: *Spectrochimica Acta Part A: Molecular and Biomolecular Spectroscopy*

Received Date: 29 November 2013
Revised Date: 25 July 2014
Accepted Date: 30 July 2014

Please cite this article as: J. Masternak, B. Barszcz, M. Hodorowicz, O.V. Khavryuchenko, A. Majka, Synthesis and physicochemical characterisation of two lead(II) complexes with O-, N-donor ligands. Lone pair functionality and crystal structure, *Spectrochimica Acta Part A: Molecular and Biomolecular Spectroscopy* (2014), doi: <http://dx.doi.org/10.1016/j.saa.2014.07.084>

This is a PDF file of an unedited manuscript that has been accepted for publication. As a service to our customers we are providing this early version of the manuscript. The manuscript will undergo copyediting, typesetting, and review of the resulting proof before it is published in its final form. Please note that during the production process errors may be discovered which could affect the content, and all legal disclaimers that apply to the journal pertain.



Synthesis and physicochemical characterisation of two lead(II) complexes with O-, N-donor ligands. Lone pair functionality and crystal structure.

Joanna Masternak^{a*}, Barbara Barszcz^a, Maciej Hodorowicz^b,
Oleksiy V. Khavryuchenko^c, Alina Majka^d

^a Institute of Chemistry, Jan Kochanowski University, 15G Świętokrzyska Str., 25-406 Kielce, Poland

^b Faculty of Chemistry, Jagiellonian University, 3 Ingardena Str., 30-060 Kraków, Poland

^c Chemistry Department, Taras Shevchenko National University of Kyiv, 64 Volodymyrska Str., Kyiv UA-01601, Ukraine

^d Institute of Physical Chemistry, Polish Academy of Sciences, 44/52 Kasprzaka Str., 01-224 Warsaw, Poland

Abstract

A dinuclear $[\text{Pb}_2(4\text{-CHO-5-MeIm})_6(\text{NO}_3)_2](\text{NO}_3)_2$ (**1**) and a polynuclear $[\text{Pb}(2\text{-pzc})_2(\text{H}_2\text{O})]_n$ (**2**) complexes (where 5(4)-carbaldehyde-4(5)-methylimidazole (5(4)-CHO-4(5)-MeIm) and pyrazine-2-carboxylic acid (2-pzcH)) have been synthesized and characterized by elemental analysis, IR spectroscopy and X-ray crystallography. Structural determination for complex **1** reveals a cationic species $[\text{Pb}(4\text{-CHO-5-MeIm})_3]^{2+}$ connected through bridging nitrate(V) ions. There are also uncoordinated nitrate ions as counterions. Complex **2** is a three-dimensional architecture consisting of Pb_6O_{12} building units. The pyrazine-2-carboxylato ligand behaves as a chelating agent and a bi-connective bridge. The coordination polyhedra around lead(II) ion could be described as a distorted dodecahedron (**1**) or monocapped trigonal prism (**2**). The luminescent properties of **1** and **2** investigated in the solid state at room temperature indicate structure-dependent photoluminescent properties. The DFT calculations and the X-ray structural data point on rather hemidirected type of coordination around Pb(II) ions of **1** and **2**.

Keywords

Lead(II) complexes, X-ray structure, Lone pair stereoactivity, Luminescence properties

Introduction

Of all p-block elements, lead(II) has a particular fascination for coordination chemists as it can adopt many different geometries in its complex. Extensive structural studies on this subject give some evidence why Pb(II) as a central ion in complexes displays such an interesting feature. The literature data mainly pointed on: (i) the effect of so-called “inert electron-pair”, which means the size and extent of the lone-pair in the coordination sphere, (ii) the broad range of coordination numbers from 2 to 12, (iii) the kind of donating ligands and their flexibility.

Moreover, the interest of coordination chemistry of Pb(II) is also motivated by the toxicity of lead and its widespread occurrence in the environment due to its numerous industrial applications [1-5]. The coordination properties of lead over other essential metal ions is crucial to understand the toxicological properties of this metal, the design of selective

* Corresponding author. Tel.: +48 (41) 349 70 39.
E-mail address: joanna.masternak@ujk.edu.pl

chelation therapy agents, and the development of efficient chelating agents for the remediation of polluted water and soil. On the other hand, lead has been used as a heavy atom derivative to solve a crystal structure of proteins, and inspection of these structures provides useful insights into the biological chemistry of Pb(II). A landmark in the field of RNA biochemistry was the crystal structure of the transfer RNA for phenylalanine (tRNAPhe) because it constituted the first crystal structure of a transfer RNA molecule and laid the foundation for the field of catalytic RNA [6,7]. Although considerably larger than both Ca(II) and Zn(II), Pb(II) can bind to both calcium- and zinc-binding sites in proteins [8-12]. In both cases, lead binds a high coordination number site than that is made up of carboxylate groups.

In view of the aforementioned, we have successfully synthesized Pb(II) coordination dimer and polymer using 5(4)-carbaldehyde-4(5)-methylimidazole (5(4)-CHO-4(5)-MeIm) and pyrazine-2-carboxylic acid (2-pzcH) as ligands, namely $[\text{Pb}_2(4\text{-CHO-5-MeIm})_6(\text{NO}_3)_2](\text{NO}_3)_2$ (**1**), $[\text{Pb}(2\text{-pzc})_2(\text{H}_2\text{O})]_n$ (**2**). To realize the one of the goal of this work we select 5(4)-CHO-4(5)-MeIm and 2-pzcH as ligands because from bioinorganic point of view, heterocyclic aldehydes and acids are of great importance as compounds containing N,O-donor atoms which can be adopted to modeling coordination environment of toxic metal ions in biological systems. Both complexes have been characterised by X-ray single crystal structure analysis. The spectral (FTIR, PL) and thermogravimetric characterisation was also performed. Additionally, a possible stereochemical activity of the lone pair in the complexes obtained has been discussed by us based on the molecular structure of the complexes provided by DFT calculations. Such investigations are very important because despite the fact that coordination environment of Pb(II) has been subjected to detailed analyses it is frequently difficult to establish a proper coordination number and geometry. According to the literature data, holo- and hemidirected geometry are two general structural types of lead(II) complexes [13,14]. But in complexes with an intermediate coordination number (6-8) the prediction is less reliable because both types of arrangement can be observed.

Experimental

Materials and physical measurements

All of the starting materials were commercially available reagents for analytical grade and were used without further purification. Lead(II) nitrate and acetate were purchased from the Merck Chemical Company, 5(4)-CHO-4(5)-MeIm and 2-pzcH from Sigma-Aldrich. Elemental analyses (C, H and N) were performed on VarioMicro Cube elemental analyzer. Infrared (FTIR) spectra were measured on Nicolet 380 spectrophotometer in the spectral range 4000-500 cm^{-1} using a KBr pellet. Thermogravimetric analyses were carried out using a TG/SDTA 851^e METTLER-TOLEDO thermobalance with Al_2O_3 crucible. The thermoanalytical curves were obtained using STAR^e System METTLER-TOLEDO software. The powder X-ray diffraction (XRD) patterns of the products of decomposition were recorded by DRON-2 using CuK_α radiation ($\lambda = 1.54178 \text{ \AA}$) over 2θ angle range 8-90°. Fluorescence spectra of solid samples were recorded with a Spex Fluorolog 3 spectrofluorometer equipped with a Quanta- ϕ integrating

sphere. In order to further clarify the origin of photoluminescence, the solid-state emission spectra of complexes and ligands were measured by varying the excitation wavelengths under the same metrical conditions.

Single crystal X-ray diffraction studies

Diffraction intensity data for single crystal of lead(II) complexes were collected at room temperature on a KappaCCD (Nonius) diffractometer with graphite-monochromated MoK α radiation ($\lambda = 0.71073 \text{ \AA}$). Corrections for Lorentz, polarization and absorption effects [15,16] were applied. The structure was solved by direct methods using SIR-92 program package [17] and refined using a full-matrix least square procedure on F^2 using SHELXL-2013 [18]. Anisotropic displacement parameters for all non-hydrogen atoms and isotropic temperature factors for hydrogen atoms were introduced. In the structure, the hydrogen atoms connected to carbon atoms were included in calculated positions from the geometry of molecules, whereas hydrogen atoms of water molecules were included from the difference maps and were refined with isotropic thermal parameters. The figures were made using DIAMOND software [19].

Quantum-chemical method

Quantum-chemical calculations were performed in the framework of density-functional theory (DFT). Hybrid three-parameter Becke Lee-Yang-Parr functional B3LYP [20] together with Ahlrichs' triple-zeta split-valence basis set augmented by Coulomb fitting (def2-TZVPP) [21] using resolution of the identity approximation [22]. Stuttgart-Dresden effective core potential (ECP) for 60 core electrons of Pb was used [23]. The ORCA *ab initio*, DFT and semiempirical SCF-MO package [24] was used for all calculations. Monomeric form of **1** with two nitrate counter-ions and truncated dinuclear part of **2** with 'outer' coordination positions saturated with hydrogen atoms were used as models for the DFT calculations. Positions of hydrogen atoms were optimized, while other atoms retained the same coordinates as determined from single-crystal X-ray analysis. Molecular orbitals were localized for analysis using Foster-Boys (spatial localization) algorithm [25].

Syntheses

Preparation of [Pb₂(4-CHO-5-MeIm)₆(NO₃)₂](NO₃)₂ (**1**)

The complex was prepared by layering method. A water solution (10 cm³) of lead(II) nitrate (1 mmol) was carefully layered over 20 cm³ of isopropanol-water (1:3, v/v) solution of 5(4)-CHO-4(5)-MeIm (3 mmol). Colourless crystals were finally formed within six weeks (at 4°C in a refrigerator). The product was collected in 39% yield. Anal. calcd (%) for C₁₅H₁₈N₈O₉Pb (661.56): C, 27.23; H, 2.74; N, 16.94; Found (%): C, 27.60; H, 2.53; N, 16.77. FTIR (cm⁻¹): 3320 (m), 3120 (w), 3066 (w), 3001 (w), 2933 (m), 2885 (m), 2857 (m), 2811 (m), 1767 (w), 1738 (w), 1651 (s), 1625 (m), 1584 (w), 1517 (w), 1446 (m), 1415 (m), 1356 (m), 1303 (s), 1251 (m), 1107 (w), 1093 (w), 1033 (m), 948 (s), 867 (w), 806 (s), 721 (m).

Preparation of [Pb(2-pzc)₂(H₂O)]_n (**2**)

The formation of the complex was accomplished by neutralization of the pyrazine-2-carboxylic acid (2-pzcH). Lead(II) nitrate (1 mmol) was dissolved in warm distilled water (10 cm³) and added to an aqueous solution (15 cm³) of sodium pyrazine-2-carboxylate (generated *in situ* by reacting (2 mmol) pyrazine-2-carboxylic acid with sodium bicarbonate (2 mmol)) under continuous stirring. The suspension was heated at 40 °C until a clear solution was obtained. The solution was cooled and left at room temperature. After five weeks the colourless crystals suitable for X-ray crystallography were obtained. Yield 31% (based on Pb(II) salt). Anal. calcd (%) for C₁₀H₈N₄O₅Pb (471.40): C, 25.48; H, 1.71; N, 11.88; Found (%): C, 25.41; H, 1.58; N, 11.82. FTIR (cm⁻¹): 3369 (m, br), 1592 (s), 1580 (s), 1522 (m), 1459 (w), 1410 (m), 1359 (s), 1319 (m), 1280 (m), 1157 (s), 1047 (m), 1026 (s), 819 (m), 789 (s), 718 (s).

Results and discussion

Description of the structures

We describe in detail the structure of [Pb₂(4-CHO-5-MeIm)₆(NO₃)₂](NO₃)₂ (**1**) and [Pb(2-pzc)₂(H₂O)]_n (**2**) complexes which were determined by X-ray crystallography. Crystal data (selected bond lengths, valence angles, hydrogen bonds) and structure refinement of these compounds are given in **Tables 1-4**.

Table 1

Table 2

Table 3

Table 4

Crystal structure of complex 1

A single crystal X-ray structural analysis shows that complex **1** consists of a neutral dimeric coordination unit which consist of [Pb₂(4-CHO-5-MeIm)₆(NO₃)₂]²⁺ cation and two free NO₃⁻ anions (see **Fig. 1**). Each lead atom is chelated by the nitrogen and oxygen atoms of three 4-carbaldehyde-5-methylimidazole ligands with Pb–N distances ranging from 2.457(3) to 2.703(3) Å and Pb–O distances of 2.596(3), 2.667(3) and 2.803(3) Å which is in the normal range and well comparable with such complexes [13 and literature cited there]. Two [Pb(4-CHO-5-MeIm)₃(NO₃)]⁺ are bridged into a centrosymmetric dimer by two bidentate bridging nitrate ligand in μ -O, O' fashion. The presence of a lone pair of the lead ion, is apparently the reason why the bridging interactions are so long. The interaction of lead(II) with oxygen atoms of nitrate anions (Pb–O(NO₃⁻) distances 2.911(4) and 3.019(3) Å) are weaker [26] but not so long as bonds in hemidirected lead(II) complexes presented in literature [27]. Simultaneously, all Pb–N and Pb–O distances are shorter than the sum of the ionic radii (3.54 Å and 3.40 Å, respectively) [28-34], therefore these Pb ions have significant first-order Pb–N and first-, second-order Pb–O interactions. In fact the coordination number of Pb(II) in this complex is eight (CN=8): six normal bonds with donor atoms of 4-CHO-5-MeIm and two “weak” Pb···O bonds of nitrite ligands. Additionally, the lone pair impact is

plainly evident in distortion of all valence angles (**Table 3**). Therefore, coordination polyhedron can be considered a pseudo-dodecahedron. Additionally, the arrangement of donor atoms suggests gaps or holes in the coordination geometry at the site of stereo-active lone pair of electrons. The coordination sphere of Pb(II) could be best described as “*pseudo-hemidirected*” (i.e., transition between hemidirected and holodirected) [35].

In the crystal structure of **1** there are intramolecular hydrogen bonds of the N-H \cdots O type formed by the imidazole N atoms as proton donors and nitrate atoms (see **Table 2**). In addition, the weak intermolecular interaction (N-H \cdots O and C-H \cdots O type), between the adjacent complex molecules are responsible for the molecular packing (**Fig. 2**).

Fig. 1.

Fig. 2.

Crystal structure of complex 2

The X-ray analysis of compound **2**, of formulation [Pb(2-pzc) $_2$ (H $_2$ O)] $_n$, revealed that it is composed of coordination polymer (**Fig. 3**). Each lead atom is chelated by two 2-pzc $^-$ ligands through the pyridine N-donor and one carboxylate oxygen atom. The bond distances associated to the chelating ligands are Pb–N 2.591(4) Å and Pb–O 2.364(3) Å and 2.585(4) Å. It is interesting to note that both 2-pzc $^-$ ligands are coordinated to the central Pb(II) ion in different bridging modes. One of the 2-pzc $^-$ anions is coordinated to two different Pb(II) ions through one of the carboxylate oxygen atoms (O(8B) $_{(-x+1,-y,-z)}$), which functions as a monoatomic bridge (μ^2 - η^2) (**Fig. 4a**). The second independent 2-pzc $^-$ ligand functions as a bridging bidentate ligand (μ^2 - η^1 : η^1) which is linked to two symmetry related Pb(II) ions *via* O(8A) and O(9A) oxygen atoms (**Fig. 4b**). Moreover, lead ion is also coordinated by oxygen atom from water molecule (Pb–O(1) bond distance 2.596(3) Å). Thus, the Pb(II) ion coordinates to four carboxylate oxygen atoms and one oxygen from water molecule. The coordination sphere of Pb(II) ion is completed by two pyridine-like nitrogen atom (N(1A) and N(1B) giving {PbN $_2$ O $_5$ } chromophore, resulting in coordination polyhedron described as distorted monocapped trigonal prism. The most interesting feature of the crystal packing is existence of mesh network which is built of two kinds of cavities: (1) the small one constructed by two lead(II) ions bridged by the carboxylate groups (Pb \cdots Pb distance 4.163 Å), (2) the bigger are built up six Pb(II) ions joined by six bidentate bridging 2-pzc $^-$ ligands, leading to the formation of a 2-D infinite network, as illustrated in **Fig. 5a** building blocks along [1 0 1] plane.

The crystal polymeric structure is stabilized by typical and trifurcated hydrogen bonds (**Fig. 5b**). A scrutiny of the structure reveals that the noncoordinating oxygen atom of the carboxylate group (O(9B) and the coordinated water as well as nitrogen atom (N(4)) from pyrazine ring are involved in C–H \cdots O and C–H \cdots N interactions. The H-bonding interactions with H \cdots O(N) distances ranging from 2.54 to 2.62 Å (**Table 2**) are observed. These can be classified as intra- and interchain interactions.

Fig. 3.

Fig. 4.

Fig. 5.

DFT calculations

Optical activity of Pb(II) compounds is often related to spatial localization of its valent *s*-orbital [12,13]. In order to check if the compound synthesized are potentially interesting for optics we have performed DFT calculations on selected structures. Such investigations are also very important for prediction of geometry around Pb²⁺ ion in complexes with intermediate coordination number (6-8) in which both holo- and hemidirected arrangement can be observed. The results are controversial: on the one hand some orbitals of Pb are significantly asymmetric - more localized in the “empty” hemisphere of the lead surrounding; on the other hand they do not have essential contributions from *s*-orbitals. The most asymmetrically localized molecular orbitals of **1** and **2** are demonstrated in **Fig. 6**, while complete data, as well as protocols of calculations can be found in Supplementary materials (**Fig. S1, S2**). One can see that there is an obvious asymmetry of the electrons localization on certain orbitals (although total electronic density around Pb atom is rather spherical). However, the contributions to those localized orbitals (25% of *s*-, 25% of *p*-, 49% of *d*-orbitals for MO#59 of **1**; 32% of *s*-, 25% of *p*-, 40% of *d*-orbitals for MO#81 of **1**; 8% of *s*-, 40% of *p*-, 51% of *d*-orbitals for MO#35 of **2**) proves that the main role in localizing of electron density in the space responsible for the potential stereoactivity of Pb(II) complexes is due to *d*-orbitals. This seems logical, since *s*-orbitals are spherical and, thus, cannot have selected direction with higher localization, while *p*-orbitals are often strongly involved into forming covalent bonds with donating atoms of ligands. Such distribution of electronic density around Pb atom of **1** and **2** point at a hemidirected type of coordination.

Fig. 6.

Spectral studies

FTIR analysis

Selected vibration bands of free ligands and their Pb(II) complexes, which are useful for determining the ligand's mode of coordination, are given in **Table 5**. In the FTIR spectra (**Fig. S3**) the $\nu_{(C=O)}$ bands of 5(4)-CHO-4(5)-MeIm appears at 1663 cm⁻¹, typical of an aldehyde group [36] and it is slightly red-shifted in complex **1** (ca. 12 cm⁻¹). A strong peak at 1458 cm⁻¹, assigned to the $\nu_{(C=N)}$ of heteroaromatic imidazole ring vibrations is also shifted to lower energy (1446 cm⁻¹). Such shifts in the mentioned bands upon coordination are consistent with bidentate coordination of the ligand through carbonyl oxygen and pyridine-like nitrogen atom of 5(4)-CHO-4(5)-MeIm. In addition, the IR spectra have presented evidence for the coordination mode of NO₃⁻. The frequency difference of the vibrations $\Delta\nu = 29$ ($\Delta\nu = 1767 - 1738$ cm⁻¹) indicate a bidentate, bridging coordination mode of nitrates in **1** [37-39]. Moreover, a characteristic band of the NO₃⁻ counterion at about

1356 cm^{-1} was observed [26]. These features are consistent with the X-ray diffraction data for complex **1**.

In the FTIR spectrum of **2** (**Fig. S3**), the strong and broad absorption band in the range of 3200-3500 cm^{-1} (max. 3369 cm^{-1}) is assigned as the characteristic peak of $\nu(\text{O-H})$ vibration from the coordinated water molecules present in the crystal structure. Moreover, the spectra of **2** confirm the structural data indicating that the carboxylic group of ligand is deprotonated. Strong absorption bands of the free 2-pzcH ligand at 1707 and 1392 cm^{-1} which correspond to the asymmetric and symmetric $\nu(\text{COOH})$ vibrations after coordination to the Pb(II) ions were shifted to lower wavenumbers and were observed at 1592, 1580 cm^{-1} and 1359, 1319 cm^{-1} , respectively. Band splitting of the stretching vibrations of the carboxylate group, suggest that 2-pzc⁻ exhibited a different coordination mode. It may function as: (a) bridging ($\mu_2\text{-}\eta^1:\eta^1$) mode and (b) bridging ($\mu_2\text{-}\eta^2$) mode (see **Fig. 4a, b**). The differences between the asymmetric and symmetric stretches of the carboxylate groups of complex **2**, $\Delta\nu = 233$ and 261 cm^{-1} , give some qualitative information which allows the correlation of the data of the infrared spectra with the coordination modes of lead(II) carboxylates (a) and (b) respectively [40-43].

Table 5

Luminescence spectra

Complexes **1**, **2** reported in this work exhibit the photoluminescence properties at room temperature in the solid-state (**Fig. 7**). The luminescent spectrum of **1** indicated an emission maximum at 575 nm upon excitation at 350 nm (**Fig. 7a**). In order to assess the emission behaviour, comparison with the corresponding spectrum of the 5(4)-CHO-4(5)-MeIm as ligand was made. The free ligand exhibited emission band with maxima at 554 nm upon excitation with the same wavelength. The red-shifted band can be assigned to metal-to-ligand charge transfer (MLCT) [44] transition with electrons being transferred from Pb^{2+} ($6s^2$) lone pair to the unoccupied π^* orbitals of 4-CHO-5-MeIm. On the other hand these bands can be derived from intra atomic transitions from the Pb(II) $6s^2$ orbital to the Pb(II) 6p orbital [45,46].

Upon replacement of the 4-CHO-5-MeIm ligand by 2-pzcH a broad emission shifted to the blue part of the spectra in complex **2** was observed. Polymer display a broad emission band with maxima at 538 nm upon excitation with wavelength of 350 nm. As shown in **Fig. 7b** the free ligand, 2-pzcH shown a broad maximum at 553 nm upon excitation with the same wavelength. Hypsochromic shift in complex **2** has the same background as was mentioned above for **1** but the emission band has a significantly stronger luminescence intensity compare to complex **1** (**Fig. 8**).

These phenomena indicate that the ligands participates in the emission of complexes and the Pb(II) monomer in comparison to polymer is a weaker emitter. That may be attributed to the coordination diversity of the lead(II) centres and the rigidity difference of these lead(II) complexes [47].

Fig. 7.

Fig. 8.*Thermogravimetric analyses*

The TG/DTG/SDTA of compounds **1**, **2** were performed on crystalline samples under an air atmosphere from 25 to 800 °C with heating rate 5° min⁻¹. The TG curve of **1** (see **Fig. 9**) has indicated that it is stable up to 154 °C. The first weight loss in the range 154-235 °C (6.56 %) is in good agreement with the calculated value (6.8%) for the decomposition of three methyl groups. The second, clear weight loss (16.49 %) between 235 and 330 °C suggests that the N₂O₅ molecules (16.32 %) vaporized. SDTA curve shows exothermic peak. Over the range 330-790 °C, the weight loss (30.44 %) should correspond to the loss of imidazole molecules (calcd 29.51 %). The total mass loss occurring up to 800 °C is in good agreement with the formation of metallic lead and gaseous products as a final residue (observed 46.51 %, calculated 47.37 %). The final solid product was identified on the basis of powder XRD studies [48].

For compound **2**, there are five obvious weight-loss steps of decomposition. The first step occurred at ca. 35-90 °C (2.8 %), corresponding to the removal of two water molecules per formula unit (3.8 % calcd). In the second one, weight loss (4.4 %) happened at 90-150 °C, which indicates that noncoordinated part of carboxylate group (4.4 %) from complex **2** was removed. The third step (31.33 %) with exothermic effect, between 150 and 400 °C suggests the defragmentation of two pyrazine rings inclusive N-donor atoms. Lastly, steps four and five, 400-800 °C, are connected with last part of organic ligand including the O-donor atoms connected with central lead(II). Assuming that the residue at 800 °C corresponds to metallic lead, the overall observed weight loss (57.85%) is in good agreement with that calculated for Pb (58.47%). Additionally, the final product was confirmed from XRD patterns [48] and identified on the basis of ICDD using XRAYAN package.

Fig. 9.**Conclusion**

In summary, the self-assembly of lead(II) salts with 5(4)-carbaldehyde-4(5)-methylimidazole (5(4)-CHO-4(5)-MeIm) and pyrazine-2-carboxylic acid (2-pzcH) affords Pb(II) coordination dimer (**1**) and polymer (**2**). Complex **1** consists of a neutral dimeric coordination unit which is constructed by [Pb₂(4-CHO-5-MeIm)₆(NO₃)₂]²⁺ cation and two free NO₃⁻ anions. The polymer features (**2**) a 3D-like network formed by the linkage of lead(II) ions and 2-pzc⁻ ligands. The both 2-pzc⁻ ligands are coordinated in different bridging modes: monoatomic (μ²-η²) or bidentate (μ²-η¹:η¹). The most interesting feature of the crystal packing is existence of mesh network constructed of two kinds of cavities: the small one (Pb...Pb distance 4.163 Å) and the bigger which is built up six Pb(II) ions joined by six bidentate bridging 2-pzc⁻ ligands. Therefore, it can be consider as promising metal-organic frameworks (MOFs).

The nonspherical distribution of ligands surrounding the lead(II) ion in **1**, **2** (pseudo-hemidirected geometry, see **Fig. 10**) results from the presence of the stereochemically active

lone electron pair. The DFT computations of the isolated complexes are in good agreement with structural results obtained by X-ray diffraction.

Based on the literature data, the Pb-O bonds lengths in complexes belongs to the first or second coordination sphere. According to R.L. Davidovich [13] the secondary bonds are mostly realised by a bridging ligands (COO^-) or NO_3^- (additionally mentioned by Hakimi [26] and Marandi [27]). In our case (**1**) this group of bonds is presented by the interaction of lead(II) with oxygen atoms of bridging nitrate anions ($\text{Pb}-\text{O}(\text{NO}_3^-)$ with distances 2.911(4) and 3.019(3) Å. Consistent with Davidovich suggestion [13] the primary coordination sphere of the Pb(II) atom can be limited to the Pb-O distance of 2.70 Å. Taking into consideration complex **2** with pyrazine-2-carboxylate as ligand, Pb(II)-O bonds (2.363-2.585 Å) belongs to the primary coordination sphere of Pb(II) atom but Pb-O(9A) bond (2.862 Å) of bridging carboxylate group belongs to the secondary sphere of metal atom.

Complexes reported in this work exhibit the photoluminescence properties at room temperature in the solid-state. The bands at 574 nm (**1**) and 638 nm (**2**) can be assigned to metal-to-ligand charge transfer (MLCT) transition.

The thermogravimetric analysis showed that complex **1** exhibited higher thermal stability in comparison to hydrated complex **2**.

Fig. 10.

Acknowledgement

We would like to thank Dr J. Karpiuk (Polish Academy of Sciences) for cooperation during data collections.

Appendix A. Supplementary material

CCDC 973041, 973040 contains the supplementary crystallographic data for **1**, **2**. These data can be obtained free of charge from The Cambridge Crystallographic Data Centre via www.ccdc.cam.ac.uk/data_request/cif. Supplementary data associated with this article can be found, in the online version, at [http...](http://...)

References

- [1] M.J. Katz, D.B. Leznoff, *J. Am. Chem. Soc.* 131 (2009) 18435-44.
- [2] H. Ahmadzadi, F. Marandi, A. Morsali, *J. Organomet. Chem.* 694 (2009) 3565-69.
- [3] M.J. Katz, H. Kaluarachchi, R.J. Batchelor, A.A. Bokov, A.-G. Ye, D.B. Leznoff, *Angew. Chem.* 119 (2007) 8960-63.
- [4] X.-F. Zhang, S. Gao, L.-H. Huo, H. Zhao, *Acta Crystallogr. Sect. A* 62 (2006) m617-19.
- [5] C.B. Murray, S. Sun, W. Gaschler, H. Doyle, T.A. Betley, C.R. Kagan, *IBM J. Res. Dev.* 45 (2001) 47-55.
- [6] E.K. Jaffe, J. Martins, J. Li, J. Kervinen, J. Roland, L. Dunbrack, *J. Biol. Chem.* 276 (2001)1531.
- [7] W.N. Lipscom, J.G. N. Reeke, J.A. Hatsuck, F.A. Quiocho, P.H. Bethge, *Philos. Trans. R. Soc. London, Ser. B* 257 (1970) 177.
- [8] H.M. Holden, I. Rayment, *Arch. Biochem. Biophys.* 291 (1991) 187.

- [9] R.B. Sutton, B.A. Davletov, A.M. Berghuis, T.C. Sudhof, S. R. Sprang, *Cell* 80 (1995) 929.
- [10] R.B. Sutton, J.A. Ernst, A.T. Brunger, *J. Cell Biol.* 147 (1999) 589.
- [11] E. K. Jaffe, *Bioenergetics and Biomembranes* 27 (1995) 169.
- [12] L. Shimoni-Livny, J.P. Glusker, C.W. Bock, *Inorg. Chem.* 37 (1998) 1853.
- [13] R.L. Davidovich, V. Stavila, D.V. Marinin, E.I. Voit, K.H. Whitmire, *Coord Chem Rev* 253 (2009) 1316–52.
- [14] M.H. Jack, M. Saeed, A.S. Ali, *Inorg. Chem.* 43 (2004) 1810.
- [15] Nonius COLLECT. Delft, The Netherlands: Nonius BV 1997-2000.
- [16] Z. Otwinowski, W. Minor, *Met. Enzymol.* 276 (1997) 307-26.
- [17] A. Altomare, G. Casarano, C. Giacovazzo, C. Guagliardi, M.C. Burla, G. Palidori, G. Camalli, *J. Appl. Crystallogr.* 27 (1994) 435-6.
- [18] G.M. Scheldrick, SHELXL-2013, Program for crystal structure refinement. Germany: University of Göttingen; 2013.
- [19] K. Brandenburg, H. Putz, Rathausgasse 30, Bonn: GbR. 1997-2000; version 3.2g.
- [20] A.D. Becke, *J. Chem. Phys.* 98 (1993) 5648.
- [21] F. Weigend, R. Ahlrichs, *Phys. Chem. Chem. Phys.* 7 (2005) 3297.
- [22] F. Neese, F. Wennmohs, A. Hansen, U. Becker, *Chem. Phys.* 356 (2009) 98–109.
- [23] B. Metz, H. Stoll, M. Dolg, *J. Chem. Phys.* 113 (2000) 2563.
- [24] F. Neese, The ORCA program system. *Wiley Interdiscip. Rev. Comput. Mol. Sci.* 2 (2012) 73-8.
- [25] D.A. Kleier, T.A. Halgren, J.H. Hall Jr., W.N. Lipscomb, *J. Chem. Phys.* 61 (1974) 3905.
- [26] M. Hakimi, B.-M. Kukovec, E. Schuh, Z. Normohammadzadeh, F. Mohr, *J. Chem Crystallogr.* 42 (2012) 180–5.
- [27] F. Marandi, I. Saghatforoush, I. Pantenburg, G. Meyer, *J. Mol. Struct.* 938 (2009) 277-82.
- [28] S.-R. Fan, L.-G. Zhu, *Inorg. Chem.* 46 (2007) 6785.
- [29] J. Yang, J.-F. Ma, Y.-Y. Liu, J.-C. Ma, S.R. Batten, *Inorg. Chem.* 46 (2007) 6542.
- [30] R.D. Hancock, J.H. Reibenspies, H. Maumela, *Inorg. Chem.* 43 (2004) 2981.
- [31] C. Platas-Iglesias, D. Esteban-Gómez, T. Enríquez-Pérez, F. Avecilla, A. Blas, T. Rodríguez-Blas, *Inorg. Chem.* 44 (2005) 2224.
- [32] K.J. Nordell, K.N. Schultz, K.A. Higgins, M.D. Smith, *Polyhedron* 23 (2004) 2161.
- [33] A.A. Soudi, F. Marandi, A. Morsali, L.-G. Zhu, *Inorg. Chem. Commun.* 8 (2005) 773.
- [34] Y.-Z. Yuan, J. Zhou, X. Liu, L.-H. Liu, K.-B. Yu, *Inorg. Chem. Commun.* 10 (2007) 475.
- [35] Y. Cho, S. Kim, S. Pyo, Y.S. Park, S.-J. Kim, H. Yun, J. Do, *Polyhedron* 29 (2010) 2105-10.
- [36] K. Nakamoto, *Infrared and Raman spectra of inorganic and coordination compounds*. 6th ed. Hoboken: Wiley; 2009.
- [37] A.B.P. Lever, E. Mantovani, B.S. Ramaswamy, *Can. J. Chem. Eng.* 49 (1971) 1957–64.
- [38] R. Alizadeh, V. Amani, *Struct. Chem.* 22 (2011) 1153-63.
- [39] C.C. Addison, D.W. Amos, D. Sutton, W.H.H. Hoyle, *J. Chem. Soc.* (1967) 808-812.
- [40] M.A.S. Goher, A.M. M. Abu-Youssef, F.A. Mautner, *Polyhedron* 15 (1996) 456.

- [41] P. Koczoń, J. Piekut, M. Borawska, R. Świsłocka, W. Lewandowski, *Spectrochim. Acta Part A* 61 (2005) 1921.
- [42] Z. Vargová, V. Zeleňák, I. Čisáková, K. Györyová, *Thermochim. Acta* 423 (2004) 149–57.
- [43] G.B. Deacon, R.J. Phillips, *Coord. Chem. Rev.* 33 (1980) 227-250.
- [44] M.J. Katz, V.K. Michaelis, P.M. Aguiar, R. Yson, H. Lu, H. Kaluarachchi, R.J. Batchelor, G. Schreckenbach, S. Kroeker, H.H. Patterson, D.B. Leznoff, *Inorg. Chem.* 47 (2008) 6353-63.
- [45] A. Vogler, H. Nikol, *Pure Appl. Chem.* 64 (1992) 1311.
- [46] P.C. Ford, A. Vogler, *Acc. Chem. Res.* 26 (1993) 220.
- [47] S. K. Dutta; M. W. Perkovic, *Inorg. Chem.* 41 (2002) 6938.
- [48] Powder Diffraction file, JCPDS: ICDD, 1601 Park Lane, Swarthmore, PA 19081, File no. 4-686.

Figure captions:

Fig. 1. Coordination arrangements of the Pb^{2+} in complex **1**.

Fig. 2. View of (a) inter- and intramolecular hydrogen bonds C-H \cdots O and N-H \cdots O type in complex **1**, (b) the packing arrangement along *c* axis.

Fig. 3. Asymmetric unit of polymer **2** with atom numbering scheme.

Fig. 4. Coordination modes of the 2-pzc⁻ ligand and carboxylate group.

Fig. 5. Part of the polymer structure exhibiting the a) macrometallocycle structural motif along [1 0 1] plane, b) hydrogen interactions between water molecule and neighboring monomeric units in complex **2**.

Fig. 6. Molecular orbitals localized on Pb atoms in **1** (MO#35) and **2** ((a) MO#59; (b) MO#81), which have the most asymmetric character.

Fig. 7. Solid-state luminescence emission spectra of complexes and free ligands (**1** (a), **2** (b), respectively) at room temperature.

Fig. 8. Comparison of the complexes **1** and **2** showing growth of the emission.

Fig. 9. TG/DTG/SDTA curves of compounds **1** and **2**.

Fig. 10. The coordination polyhedra around Pb^{2+} ion in the complexes.

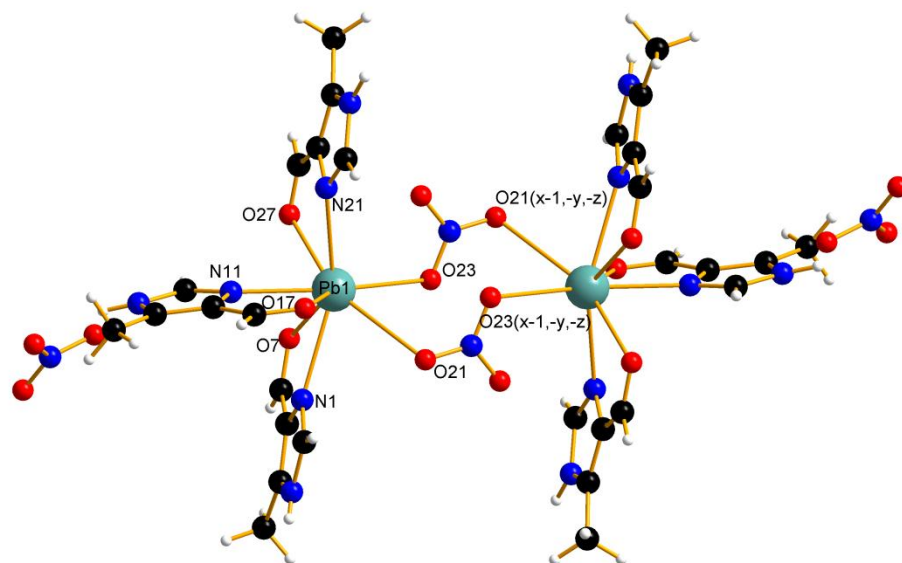


Fig. 1. Coordination arrangements of the Pb²⁺ in complex 1.

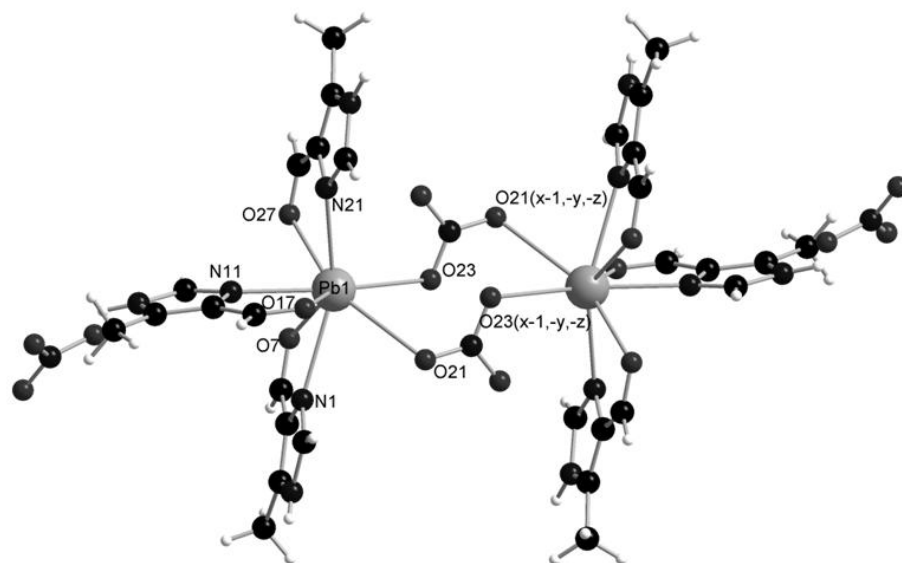


Fig. 1. Coordination arrangements of the Pb²⁺ in complex 1.

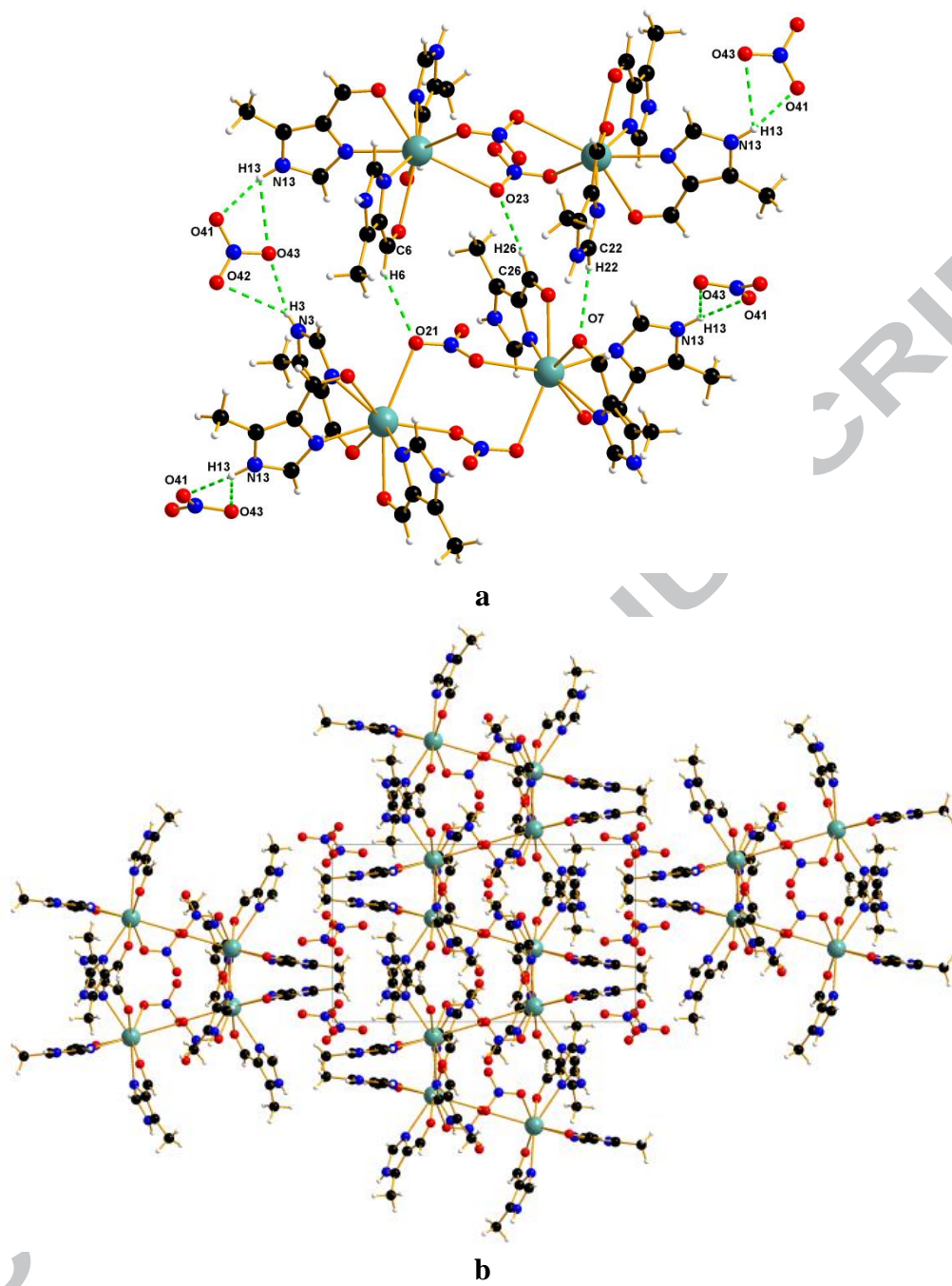


Fig. 2. View of (a) inter- and intramolecular hydrogen bonds C-H...O and N-H...O type in complex **1**, (b) the packing arrangement along *c* axis.

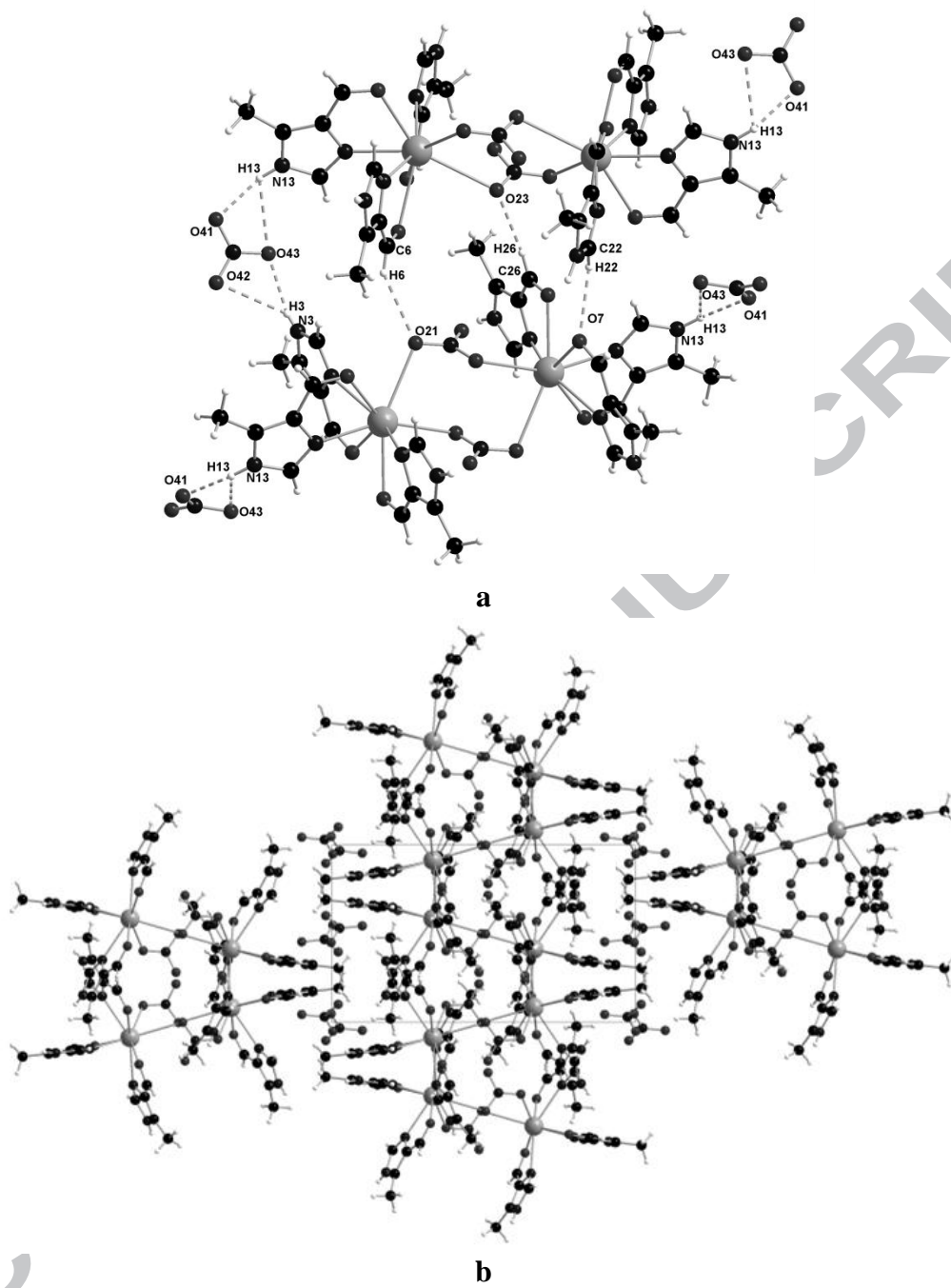


Fig. 2. View of (a) inter- and intramolecular hydrogen bonds C-H...O and N-H...O type in complex **1**, (b) the packing arrangement along *c* axis.

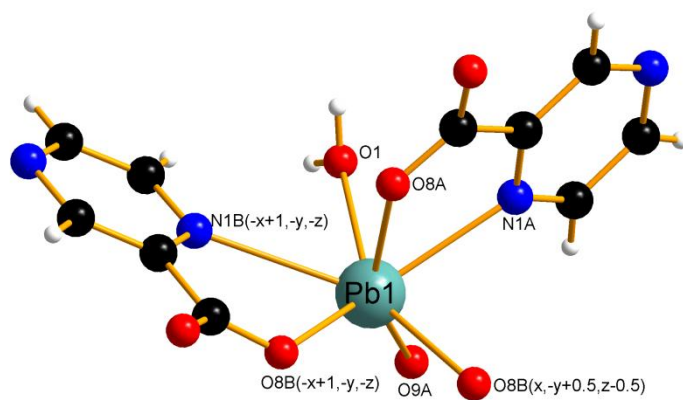


Fig. 3. Asymmetric unit of polymer **2** with atom numbering scheme.

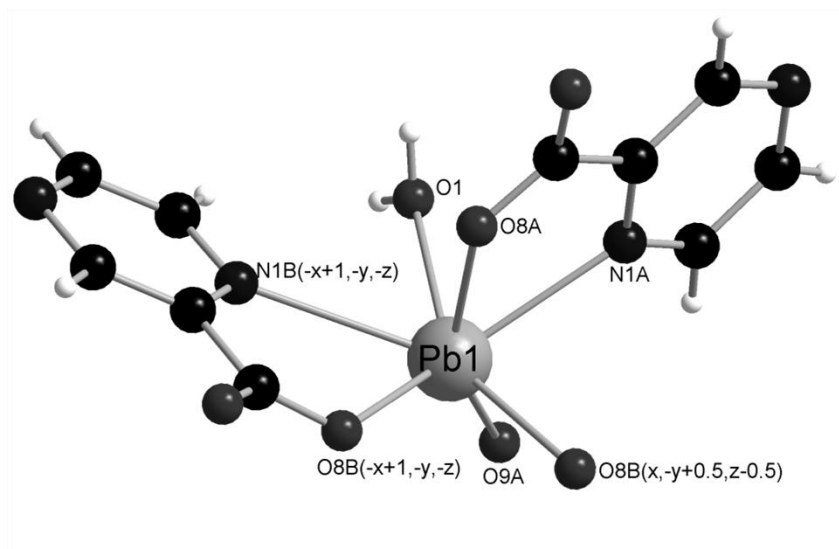


Fig. 3. Asymmetric unit of polymer **2** with atom numbering scheme.

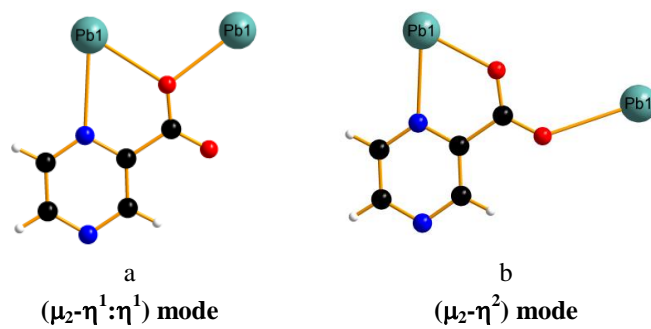


Fig. 4. Coordination modes of the 2-pzc⁻ ligand and carboxylate group.

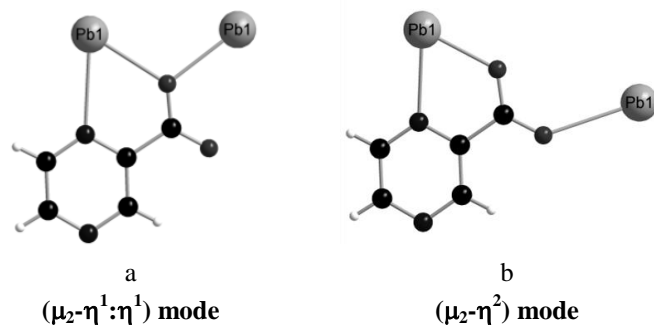


Fig. 4. Coordination modes of the 2-pzc⁻ ligand and carboxylate group.

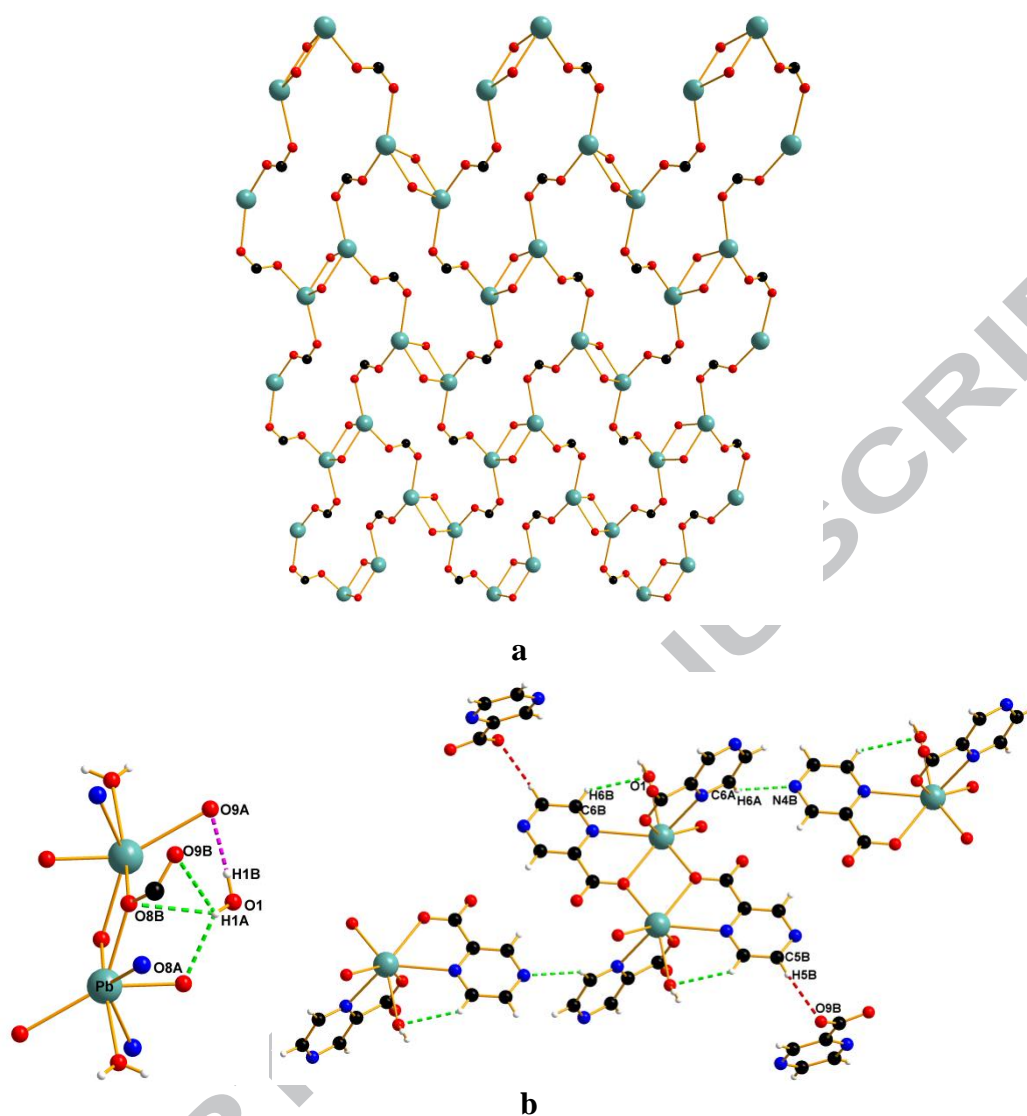


Fig. 5. Part of the polymer structure exhibiting the a) macrometallocycle structural motif along [1 0 1] plane, b) hydrogen interactions between water molecule and neighboring monomeric units in complex 2.

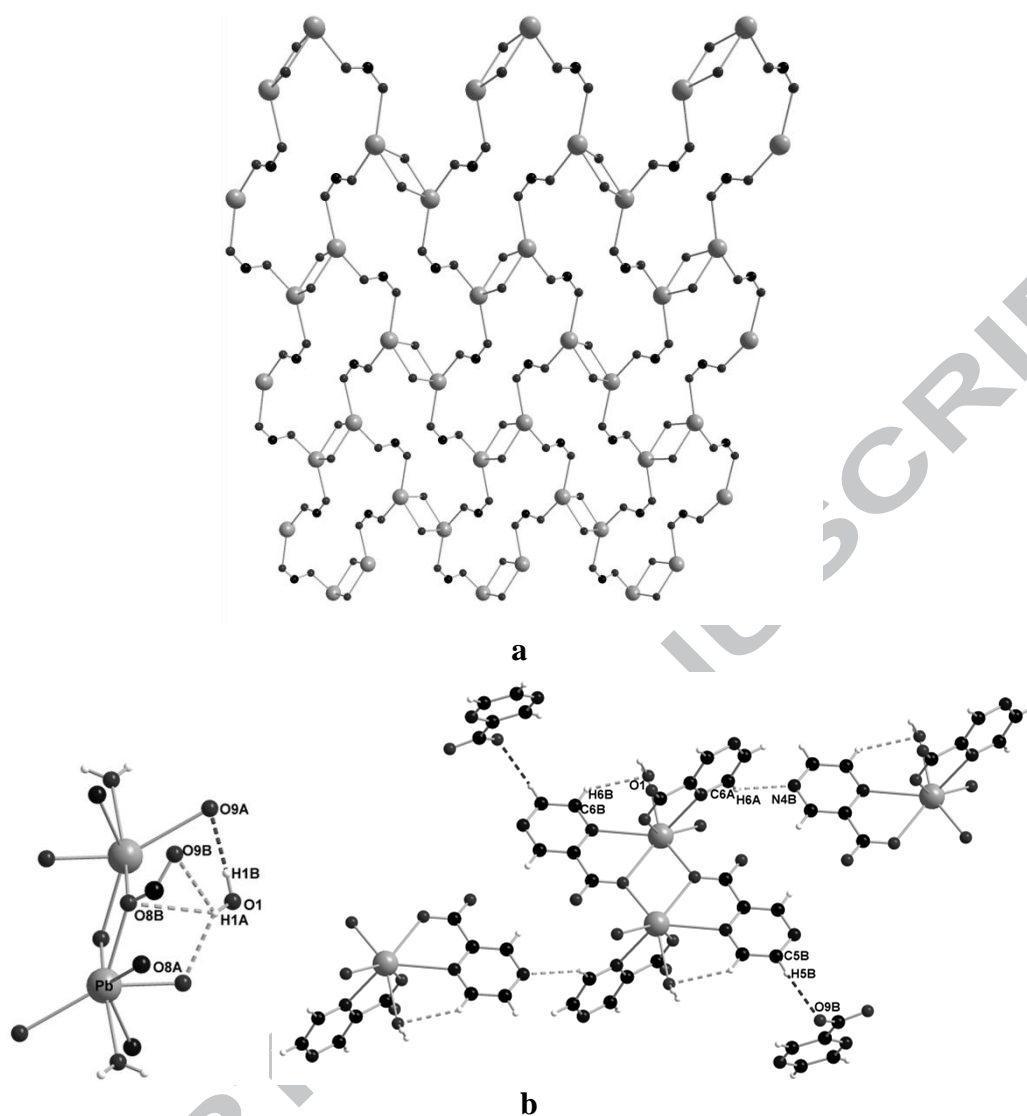


Fig. 5. Part of the polymer structure exhibiting the a) macrometallocycle structural motif along [1 0 1] plane, b) hydrogen interactions between water molecule and neighboring monomeric units in complex 2.

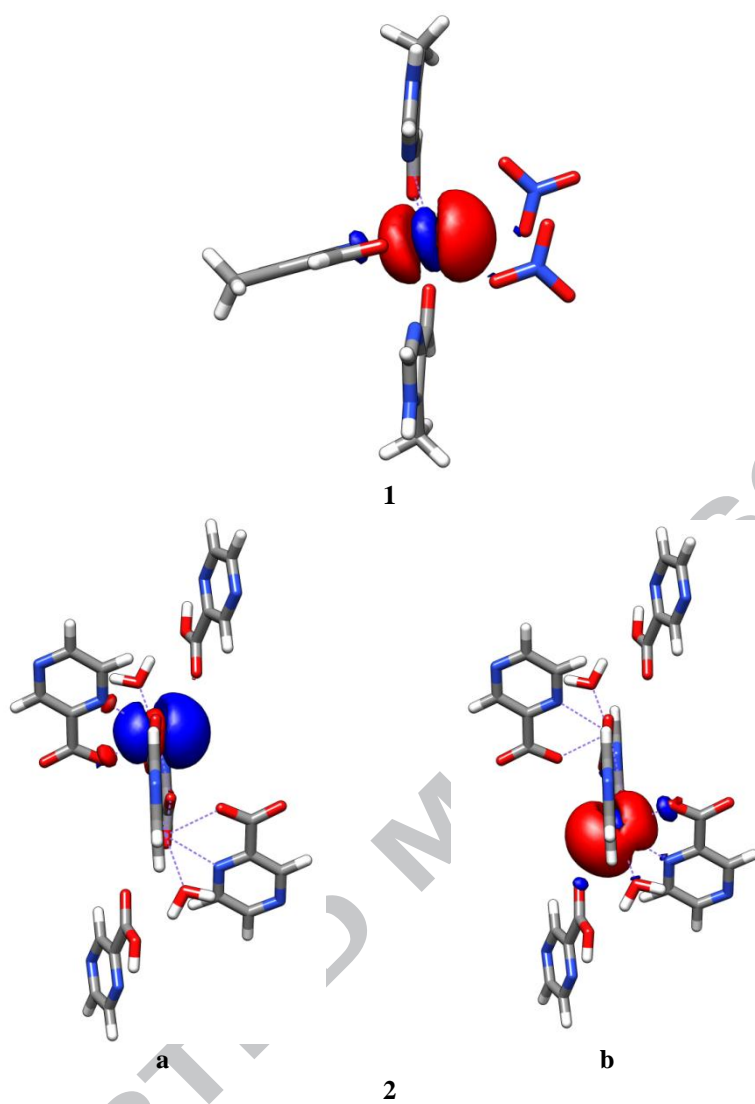


Fig. 6. Molecular orbitals localized on Pb atoms in **1** (MO#35) and **2** ((a) MO#59; (b) MO#81), which have the most asymmetric character.

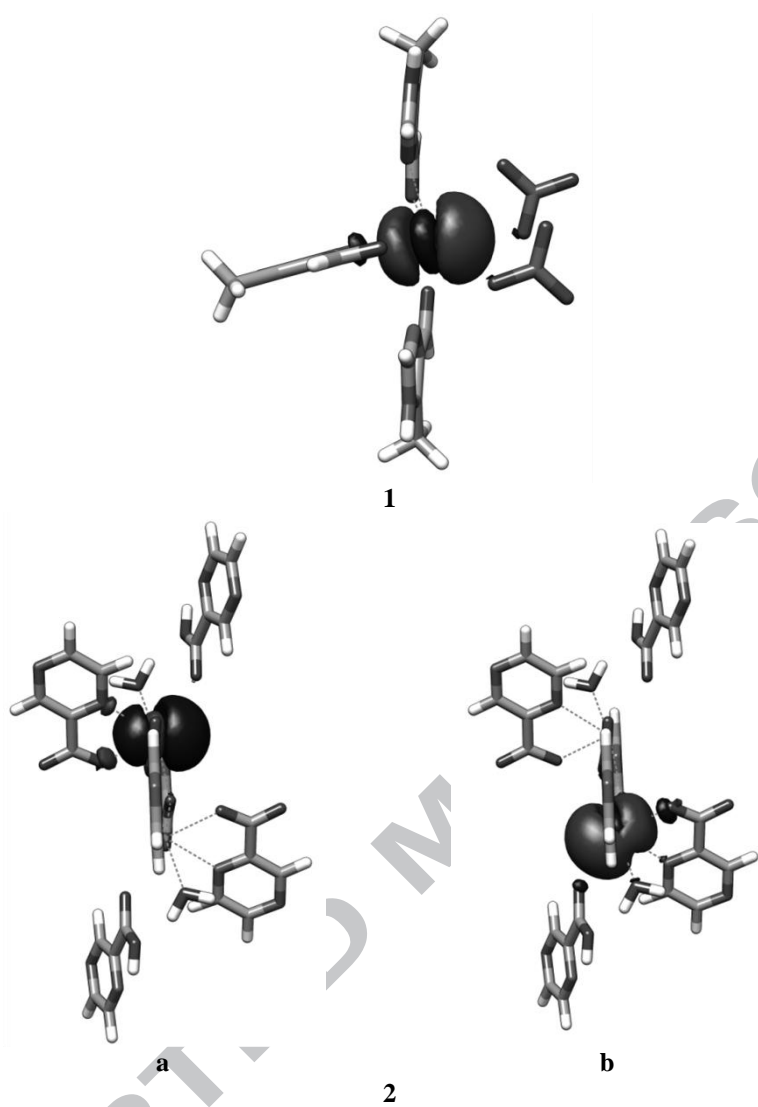


Fig. 6. Molecular orbitals localized on Pb atoms in **1** (MO#35) and **2** ((a) MO#59; (b) MO#81), which have the most asymmetric character.

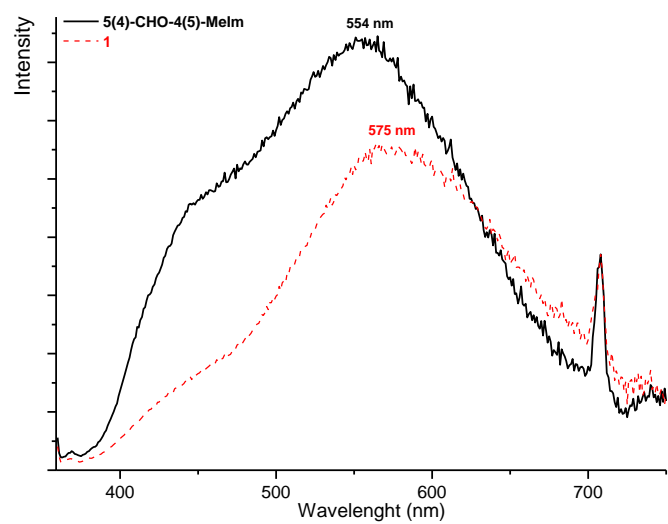
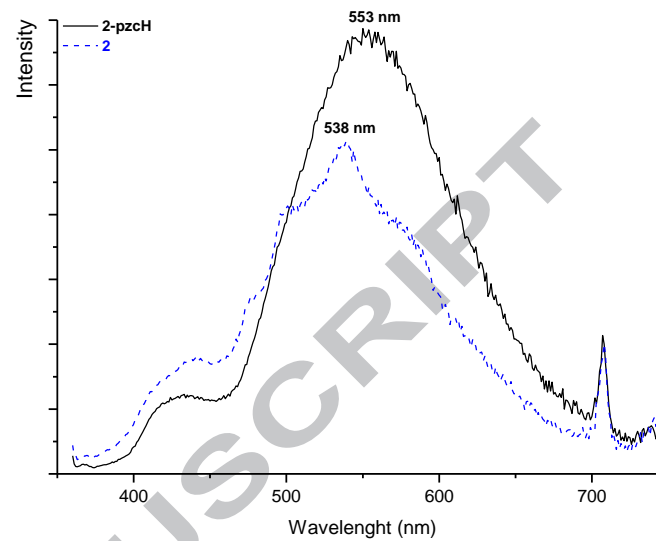
**a****b**

Fig. 7. Solid-state luminescence emission spectra of complexes and free ligands (**1** (a), **2** (b), respectively) at room temperature.

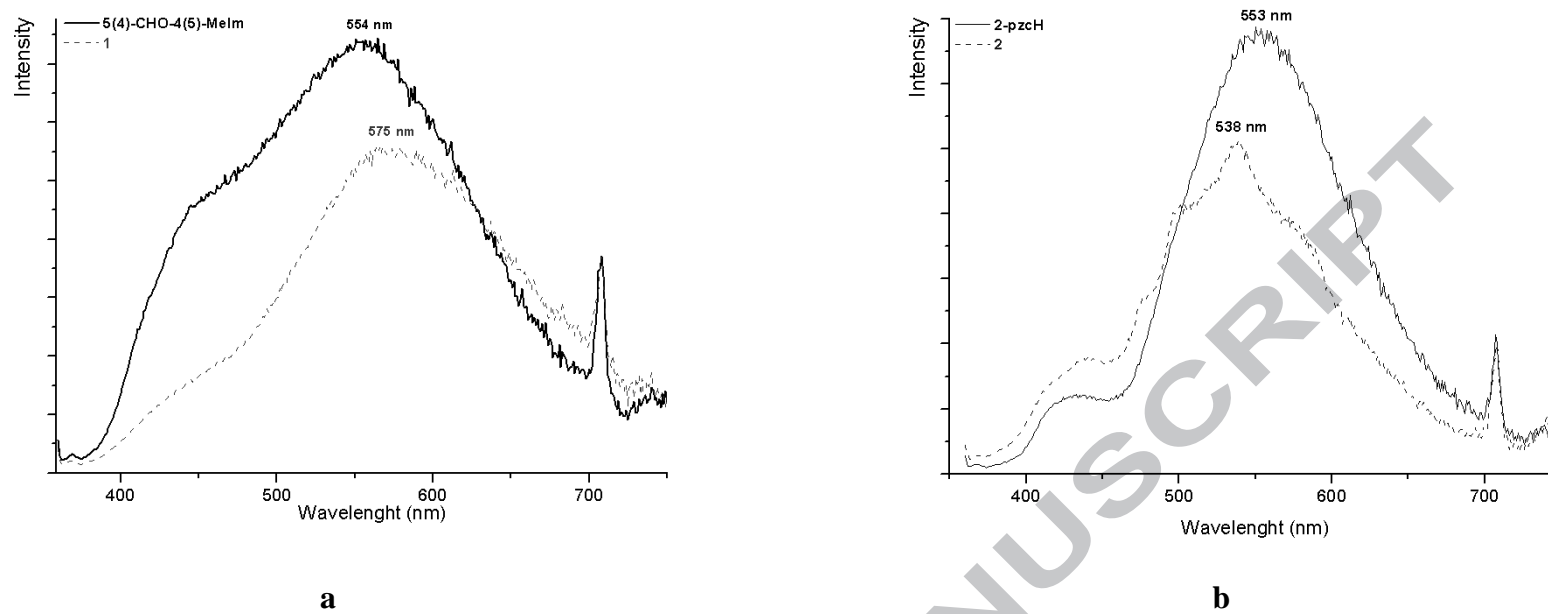


Fig. 7. Solid-state luminescence emission spectra of complexes and free ligands (**1** (a), **2** (b), respectively) at room temperature.

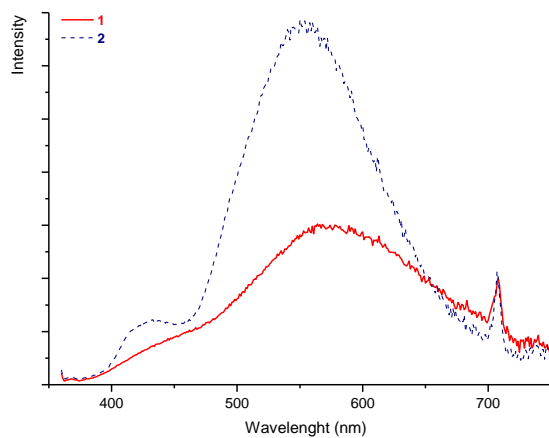


Fig. 8. Comparison of the complexes **1** and **2** showing growth of the emission.

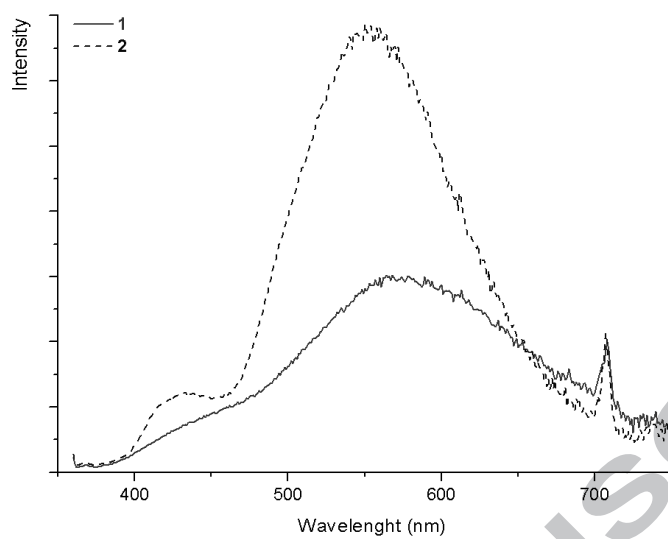
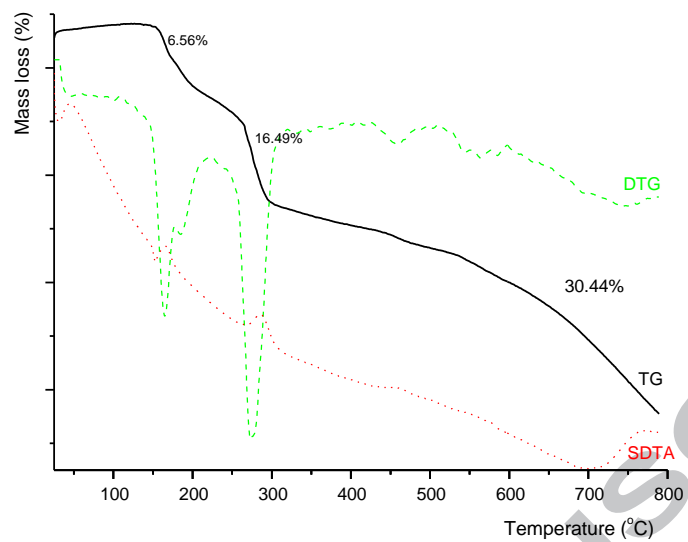
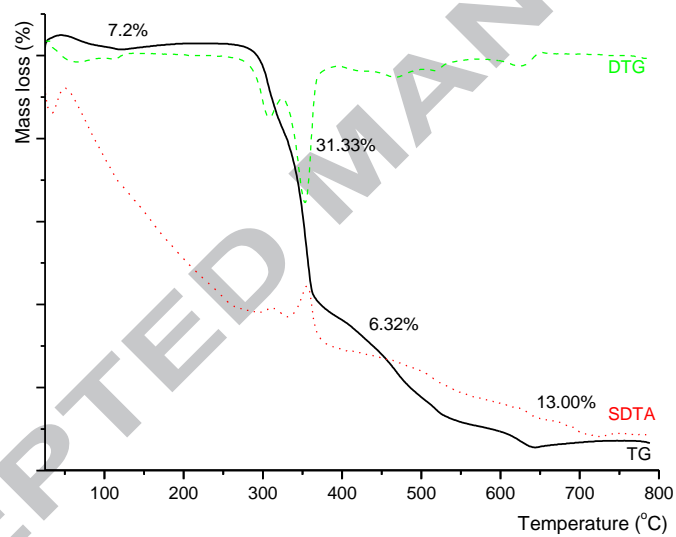


Fig. 8. Comparison of the complexes **1** and **2** showing growth of the emission.

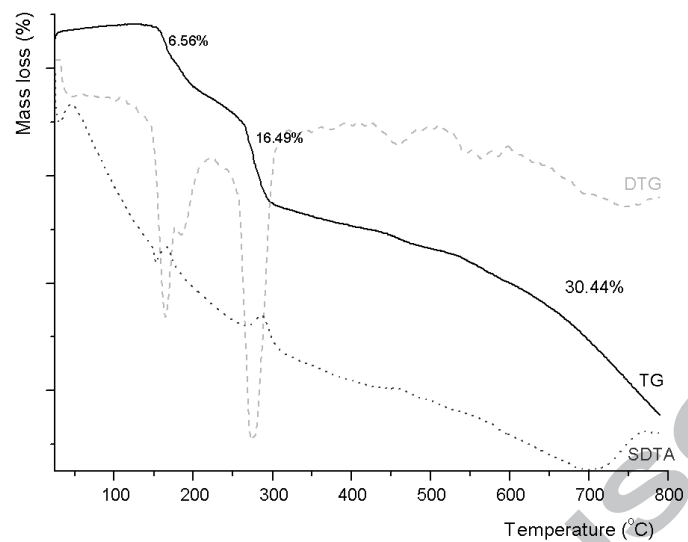
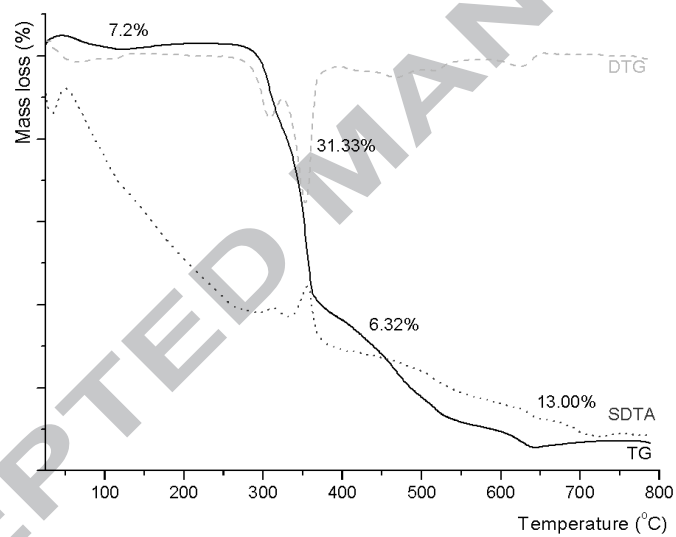


a



b

Fig. 9. TG/DTG/SDTA curves of compounds **1** (a) and **2** (b).

**a****b****Fig. 9.** TG/DTG/SDTA curves of compounds **1** (a) and **2** (b).

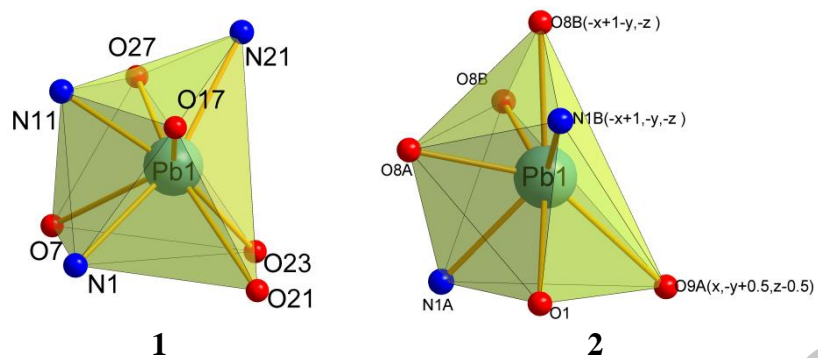


Fig. 10. The coordination polyhedra around Pb^{2+} ion in the complexes.

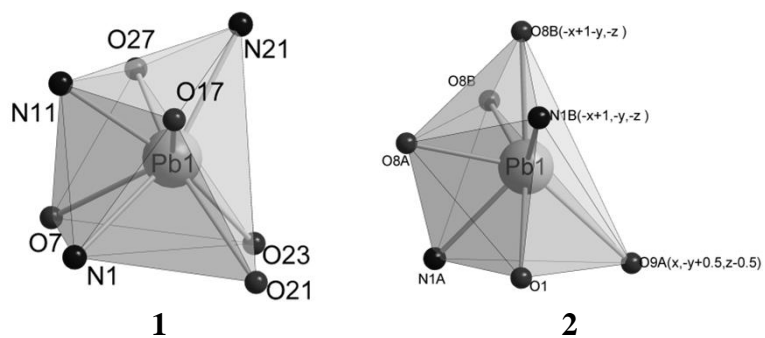


Fig. 10. The coordination polyhedra around Pb^{2+} ion in the complexes.

Table 1 Crystal data and structure refinement for **1** and **2**.

	1	2
Empirical formula	PbC ₃₀ H ₃₆ N ₁₆ O ₁₈	PbC ₁₀ H ₈ N ₄ O ₅
Formula weight	1323.14	471.39
Temperature (K)	293(2)	293(2)
Wavelength (Å)	0.71073	0.71073
Crystal system, space group	Monoclinic, P2 ₁ /c	Monoclinic, P2 ₁ /c
Unit cell dimensions	a = 17.0132(3) Å α = 90 ° b = 9.6161(2) Å β = 104.354(1) ° c = 13.5743(2) Å γ = 90 °	a = 11.147(5) Å α = 90 ° b = 10.426(5) Å β = 114.456(5) ° c = 11.712(5) Å α = 90 °
Volume (Å ³)	2151.44(7)	1239.0(1)
Z, Calculated density (Mg/m ³)	2, 2.042	4, 2.516
F(000)	1272	872
Crystal size (mm)	0.30x0.30x0.25	0.20x0.19x0.16
Theta range for data collection (°)	3.70-27.47	2.73-27.489
Index ranges	-22 ≤ h ≤ 21, -12 ≤ k ≤ 12, -17 ≤ l ≤ 17	-14 ≤ h ≤ 14, -13 ≤ k ≤ 13, -15 ≤ l ≤ 15
Reflections collected/unique/observed [R _{int}]	4925/4252 [R _{int} =0.0244]	2834/2424 [R _{int} =0.0308]
Completeness to 2θ (%)	27.48 (99.8)	27.485 (99.8)
Absorption correction		Semi-empirical from equivalents
Max. and min. transmission	0.21 and 0.25	0.171 and 0.219
Refinement method		Full-matrix least-squares on F ²
Data/restraints/parameters	4925/0/301	2833/3/189
Goodness-of-fit on F ²	1.065	1.064
Final R indices [I>2σ(I)]	R ₁ = 0.0233, wR ₂ = 0.0530	R ₁ = 0.0222, wR ₂ = 0.0497
R indices (all data)	R ₁ = 0.0296, wR ₂ = 0.0550	R ₁ = 0.0287, wR ₂ = 0.0515
Largest differences in peak and hole (e/Å ⁻³)	0.710 and -1.541	0.536 and -1.536

Table 2 Bond lengths (Å) for **1** and **2**.

1		2	
Pb(1)-N(11)	2.457(3)	Pb(1)-O(8A)	2.363(3)
Pb(1)-N(21)	2.618(3)	Pb(1)-O(8B)	2.515(3)
Pb(1)-O(27)	2.595(2)	Pb(1)-O(8B) ^I	2.585(3)
Pb(1)-O(17)	2.666(3)	Pb(1)-N(1A)	2.593(3)
Pb(1)-N(1)	2.703(3)	Pb(1)-O(1) _{H₂O}	2.599(4)
Pb(1)-O(7)	2.803(3)	Pb(1)-O(9A) ^{II}	2.862(5)
Pb(1)-O(21) _{NO₃⁻}	2.910(4)	Pb(1)-N(1B) ^I	2.810(3)
Pb(1)-O(23) _{NO₃⁻}	3.016(3)		

Symmetry transformations used to generate equivalent atoms for **2**: ^I -x+1, -y, -z; ^{II} x, -y+1/2, z-1/2;

ACCEPTED MANUSCRIPT

Table 3 Valence angles (°) for **1** and **2**.

1		2	
N(11)-Pb(1)-O(27)	73.91(8)	O(8A)-Pb(1)-O(8B)	81.99(11)
N(11)-Pb(1)-N(21)	83.55(9)	O(8A)-Pb(1)-O(8B)	74.86(10)
O(27)-Pb(1)-N(21)	65.59(8)	O(8B)-Pb(1)-O(8B)	70.54(11)
N(11)-Pb(1)-O(17)	65.29(8)	O(8A)-Pb(1)-N(1A)	65.62(10)
O(27)-Pb(1)-O(17)	126.22(8)	O(8B)-Pb(1)-N(1A)	81.83(10)
N(21)-Pb(1)-O(17)	76.12(8)	O(8B)-Pb(1)-N(1A)	134.32(10)
N(11)-Pb(1)-N(1)	72.80(9)	O(8A)-Pb(1)-O(1)	87.92(12)
O(27)-Pb(1)-N(1)	124.41(8)	O(8B)-Pb(1)-O(1)	151.50(12)
N(21)-Pb(1)-N(1)	148.37(9)	O(8B)-Pb(1)-O(1)	132.09(11)
O(17)-Pb(1)-N(1)	75.05(9)	N(1A)-Pb(1)-O(1)	69.74(12)
		O(9A) ^{II} -Pb(1)-O(8A)	149.82(10)
		O(9A) ^{II} -Pb(1)-N(1B) ^I	118.19(11)
		O(9A) ^{II} -Pb(1)-N(1A)	85.26(11)
		O(9A) ^{II} -Pb(1)-O(8B)	102.34(10)
		O(9A) ^{II} -Pb(1)-O(8B) ^I	134.99(11)
		O(9A) ^{II} -Pb(1)-O(1)	74.07(12)

Symmetry transformations used to generate equivalent atoms for **2**: ^I -x+1, -y, -z; ^{II} x, -y+1/2, z-1/2;

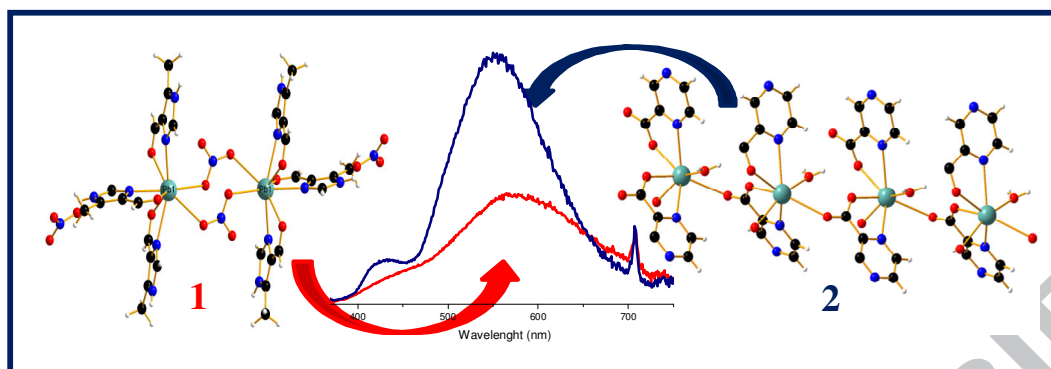
Table 4 Hydrogen bonds for **1** and **2** (Å and °).

Compound	D-H...A	(D-H) (Å)	(H...A) (Å)	(D...A) (Å)	<(DH...A) (°)
1	N(13)-H(13) ... O(41)	0.89	2.02	2.887(4)	163.7
	N(13) H(13) ... O(43)	0.89	2.58	3.052(4)	113.8
	N(3) ^I -H(3) ... O(42)	0.70	2.66	3.224(5)	138.8
	N(3) ^I -H(3) ... O(43)	0.70	2.14	2.821(4)	164.6
	C(6)-H(6) ... O(21) ^I	0.93	2.60	3.424(5)	148.2
	C(8)-H(8B) ... O(42) ^{II}	0.96	2.52	3.458(5)	164.2
	C(22) ^{III} -H(22) ... O(7) ^{IV}	0.93	2.52	3.213(5)	131.1
	N(23) ^{II} -H(23) ... O(22) ^V	0.92	2.10	2.918(5)	147.2
	C(26) ^V -H(26) ... O(23)	0.93	2.33	3.253(4)	171.0
2	C(6A)-H(6A) ... N(4B) ^I	0.93	2.62	3.318(6)	132.7
	C(5B)-H(5B) ... O(9B) ^{II}	0.93	2.54	3.463(6)	174.2
	C(6B)-H(6B) ... O(1) ^{III}	0.93	2.61	3.197(6)	121.9
	O(1)-H(1B) ... O(9A)	0.849(2)	2.16(3)	2.956(5)	155(6)
	O(1)-H(1A) ... O(8A) ^{IV}	0.86(2)	2.31(1)	2.817(5)	118(9)
	O(1)-H(1A) ... O(8B) ^V	0.86(2)	2.61(8)	3.276(5)	135(9)
	O(1)-H(1A) ... O(9B) ^V	0.86(2)	2.60(8)	3.067(5)	115(7)

Symmetry transformations used to generate equivalent atoms for (1): ^I $x, -y+1/2, z+1/2$ ^{II} $-x, y+1/2, -z+1/2$ ^{III} $-z-x+1, -y, -z$ ^{IV} $-x+1, y+1/2, -z+1/2$ ^V $-x+1, -y+1$; (2) ^I $-x+2, -y, -z$ ^{II} $-x+2, -y+1, -z$ ^{III} $-x+1, -y, -z$ ^{IV} $x, -y+1/2, -z-1/2$ ^V $-x+1, y+1/2, -z-1/2$;

Table 5 Wavenumbers (cm^{-1}) and assignments of selected bands occurring in the IR spectra of ligands and complexes.

Compound	$\nu(\text{OH})$	$\nu(\text{NH})$	$\nu(\text{C}=\text{O})$	$\nu(\text{COOH})$	$\nu_{\text{as, s}}(\text{COO}^-)$	$\nu(\text{C}=\text{C}, \text{C}=\text{N})$	$\nu(\text{NO}_3^-)$
5(4)-CHO- 4(5)-Melm	-	2928	1663	-	-	1582, 1458	-
1	-	2933	1651	-	-	1584, 1446	1415 1767, 1736, ($\Delta=29$) 1356
2-pzcH	-	-	1652	1714, 1371	-	1571, 1484	-
2	3369 ν b	-	-	-	1592, 1580, 1359, 1319 ($\Delta=233, \Delta=261$)	1580, 1449	-



ACCEPTED MANUSCRIPT

- Dimeric and polymeric Pb(II) complexes with chelating ligands has been synthesized.
- IR, PL, X-ray investigation show interesting geometry and luminescence properties.
- DFT data support the lone pair influence on holodirected arrangement of Pb(II).
- Decomposition of the complexes does not lead to oxide phases but to the metallic Pb.

ACCEPTED MANUSCRIPT